Journal of Coordination Chemistry
Publication details, including instructions for authors and subscription information:
http://www.tandfonline.com/loi/gcoo20

Study about quinolone antibacterial agent modifying the Keggin polyoxotungstates

Jingquan Sha [a], Longjiang Sun [a], Erlin Zheng [a], Hongbin Qiu [a], Mingyuan Liu [a], Hong Zhao [a] & Huan Yuan [a]

[a] The Provincial Key Laboratory of Biological Medicine Formulation, School of Pharmacy, Jiamusi University, Jiamusi, P.R. China

Accepted author version posted online: 16 Jan 2013.Published online: 25 Feb 2013.

To cite this article: Jingquan Sha, Longjiang Sun, Erlin Zheng, Hongbin Qiu, Mingyuan Liu, Hong Zhao & Huan Yuan (2013) Study about quinolone antibacterial agent modifying the Keggin polyoxotungstates, Journal of Coordination Chemistry, 66:4, 602-611, DOI: 10.1080/00958972.2013.765950

To link to this article: http://dx.doi.org/10.1080/00958972.2013.765950

Journal of Coordination Chemistry
Vol. 66, No. 4, 20 February 2013, 602–611

Study about quinolone antibacterial agent modifying the Keggin polyoxotungstates

JINGQUAN SHA, LONGJIANG SUN, ERLIN ZHENG, HONGBIN QIU*, MINGYUAN LIU, HONG ZHAO and HUAN YUAN

The Provincial Key Laboratory of Biological Medicine Formulation, School of Pharmacy, Jiamusi University, Jiamusi, P.R. China

(*Received 6 August 2012; in final form 5 November 2012*)

Three new quinolone drug molecules modifying Keggin polyoxometalate compounds have been synthesized under hydrothermal conditions and structurally characterized. Single-crystal X-ray diffraction analysis shows that Keggin clusters modified by $[Cu_2(Enro)_3H_2O]^{4+}$ subunits result in formation of dimer $\{[Cu_2(Enro)_3H_2O][SiW_{12}O_{40}]\}_2$ in **1**; in **2**, Keggin clusters are modified by two $[Cu(Norf)_2]^{2+}$ subunits in the symmetrical coordinated mode, and then, discrete $[Cu_2(Norf)_4][SiW_{12}O_{40}]$ is obtained; in **3**, Keggin clusters are fused together via $[Ni(Enro)_2]^{2+}$ subunits giving the 1D drug-polyoxometalates (POMs) hybrid chain. Antitumor activities *in vitro* show that **3** exhibits good antitumor activity, while **1** and **2** and their parent SiW_{12} show no anti-SGC7901 or anti-SMMC7721 activities, indicating that the antitumor activities rest on differences of metal ions, differently affecting electron transfer between quinolone and POMs.

Keywords: Polyoxometalate; Quinolone; Antitumor activity; Copper; Nickel

1. Introduction

Polyoxometalates (POMs) are metal oxygen anion clusters, oligomeric aggregates of metal cations (usually d^0 species V(V), Nb(V), Ta(V), Mo(VI), and W(VI)) bridged by oxygens [1–4]. Because of versatile structures and numerous applications in catalysis, materials science, magnetism, and medicine [5–9], POMs have become a growing and appealing area in multifunctional hybrid chemistry. Especially, as antitumor, antiviral, and antibacterial inorganic agents, POMs are attractive for applications in medicine. Unfortunately, when summarizing the applications of POMs in medicine, we find that the main problems that prevent the application of POMs in medicine are low hydrolytic stability and, in particular, low selectivity (accumulation in the reticuloendothelial system). Additionally, the toxicity of POMs is strongly dependent on the structure, comprising low-toxic POMs ($[SiW_{12}O_{40}]^{4-}$, $[PW_{12}O_{40}]^{3-}$) and high-toxic compounds, such as HPA-23 [10]. Nevertheless, researchers familiar with POMs have been investigating the possibilities of their antitumor, antiviral, and antibacterial activity for the following reasons: (1) nearly every molecular property (polarity, redox potentials, surface charge distribution, shape, and

*Corresponding author. Email: shajq2002@126.com

ISSN 0095-8972 print/ISSN 1029-0389 online
http://dx.doi.org/10.1080/00958972.2013.765950

acidity) that impacts the recognition and reactivity of POMs with target biological macromolecules can be altered and (2) the surface of POMs can be modified to enable design of multifunctional compounds by covalent attachment of organic groups. So introduction of organic components or their coordination polymers into the POM surface have been widely studied, with the most intriguing area the development of hybrid-based POMs modified by biologically active molecules, such as amino acid-functionalized POMs [11,12], fluorouracil-containing $[BW_{12}O_{40}]^{5-}$ [13], surfactant, and dendritic-encapsulated clusters, as well as starch and liposome-encapsulated POMs [14,15].

Quinolones, quinolonecarboxylic acids or 4-quinolones, are a group of synthetic antibacterial agents containing a 4-oxo-1,4-dihydroquinoline skeleton (scheme 1(a)). Enrofloxacin (Enro) and Norfloxacin (Norf) (scheme 1(b) and (c)), third-quinolone antimicrobial drugs and fluoro-quinolone carboxylic acid, are effectives against gram-positive and Gram-negative bacteria through inhibition of their DNA gyrase [16]. Previously, quinolones [17–19] modifying POMs have been reported by our group [20–22], and the results suggest that the introduction of quinolones/TM-quinolones onto the polyoxoanion surface can affect their antitumor activities. Many factors, such as the properties of TM ions, the donor characters of nitrogens and oxygens and coordination environment of POMs, play important roles in properties of the final products. Currently, it is difficult to propose definitive reasons that each product generates a different result. Further efforts are necessary on the TM-drugs-POMs reaction system to explore the possible effect of drug molecules modifying POM clusters.

We have chosen Keggin POMs ($[SiW_{12}O_{40}]^{4-}$) as modules, and Enro and Norf as modifiers with Cu and Ni as metal centers, to constitute drug molecules modifying POMs. It is hoped that pendent TM-drug groups could be used to modulate POMs' bioavailabilities and increase recognition of key substructures in target biomacromolecules. Herein, we report three hybrid compounds based on $[SiW_{12}O_{40}]^{4-}$, $[Cu_2(Enro)_3H_2O][SiW_{12}O_{40}]\cdot H_2O$ (**1**), $\{[Cu(Norf)_2]\}_2[SiW_{12}O_{40}]$ (**2**), and $H_2[Ni(Enro)_2][SiW_{12}O_{40}]\cdot(Enro)_2\cdot 2H_2O$ (**3**). The antitumor activities rest on differences of metal ions with different effects of electron transfer between quinolone and POMs.

2. Experimental

2.1. *Materials and methods*

All reagents were purchased commercially and used without purification. Elemental analyzes were performed on a Perkin-Elmer 2400 CHN Elemental Analyzer (C, H, and N) and on a Leaman inductively coupled plasma spectrometer (Cu and Ni). IR spectra were

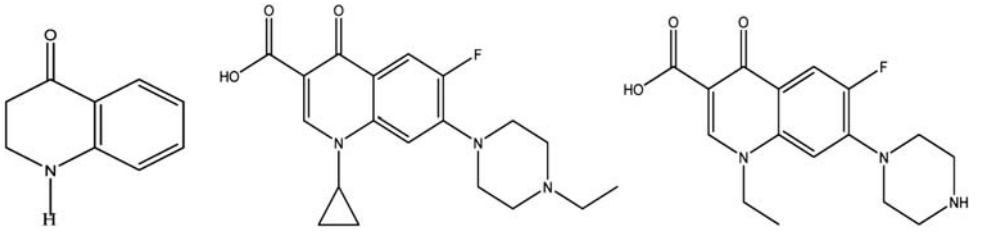

Scheme 1. Molecular structure of the 4-oxo-1,4-dihydroquinoline skeleton (a), Enrofloxacin (b), and Norfloxacin (c).

obtained on an Alpha Centaurt FT/IR spectrometer with KBr pellets from 400 to 4000 cm^{-1}. TG-DTA analyzes were performed on a Perkin-Elmer TGA7 instrument in flowing air with a heating rate of 10 °C min^{-1}. XRPD patterns were obtained with a Rigaku D/max 2500 V PC diffractometer with Cu-Kα radiation; the scanning rate is 4° s^{-1} with 2θ ranging from 5° to 40°.

2.2. *Syntheses*

2.2.1. $[Cu_2(Enro)_3H_2O][SiW_{12}O_{40}]\cdot H_2O$ (1). A mixture of $H_4SiW_{12}O_{40}$ (280 mg), $Cu(CH_3COO)_2{\cdot}2H_2O$ (50 mg), Enro (45 mg), $NaHCO_3$ (10 mg) and H_2O (10 mL) was stirred for 1 h in air. The pH was then adjusted to 4.5 with 1 M CH_3COOH, and the mixture was transferred to an 18 mL Teflon-lined reactor. After 6 days heating at 160 °C, the reactor was slowly cooled to room temperature over a period of 16 h. Green block crystals of **1** were filtered, washed with water and dried at room temperature. $C_{57}H_{70}Cu_2F_3N_9O_{51}SiW_{12}$ (4115.59): Calcd. C 16.62, H 1.70, N 3.06, Cu 3.08%; Found: C 16.59, H 1.81, N 3.05, Cu 3.07%.

2.2.2. $\{[Cu(Norf)_2]\}_2[SiW_{12}O_{40}]$ (2). Compound **2** was prepared in a manner similar to that described for **1**, except Norf replaced Enro. Green crystals were obtained. $C_{64}H_{72}Cu_2F_4N_{12}O_{52}SiW_{12}$ (4278.70): Calcd. C 17.95, H 1.68, N 3.93, Cu 2.96%; Found: C 17.69, H 1.71, N 3.91, Cu 2.96%.

2.2.3. $H_2[Ni(Enro)_2][SiW_{12}O_{40}]\cdot(Enro)_2\cdot 2H_2O$ (3). Compound **3** was prepared in a manner similar to that described for **1**, except $Ni(CH_3COO)_2$ replaced $Cu(CH_3COO)_2$. Light green crystals were obtained. $C_{76}H_{94}F_4N_{12}NiO_{54}SiW_{12}$ (4408.60): Calcd. C 20.68, H 2.13, N 3.81, Ni 1.33%; Found: C 20.67, H 2.21, N 3.79, Ni 1.31%.

2.3. *X-ray crystallographic study*

Crystal data for **1–3** were collected on a Bruker SMART-CCD diffractometer with Mo-Kα monochromatic radiation ($\lambda = 0.71069$ Å) at 293 K. All structures were solved by direct methods and refined by full matrix least-squares on F^2 using SHELXTL crystallographic software package [23]. All non-hydrogen atoms were refined anisotropically. Positions of hydrogens on carbon were calculated theoretically. The crystal data and structure refinements of **1–3** are summarized in table 1. Selected bond lengths and angles for **1–3** are listed in tables S1–S3.

2.4. *Antitumor activity studies*

The antitumor activities of **1–3** and their parent anion on SGC7901 and SMMC7721 cells were tested by the MTT experiment [24]. MTT, 3-[4,5-dimethylthiazol-2-yl]-2.5-diphenyltetrazolium bromide, also known as thiazolyl blue, is a dye which can accept a hydrogen. Surviving tumor cells are able to reduce the yellow MTT to an insoluble blue formazan in water, whereas dead tumor cells do not possess this capability. The formazan product is dissolved in DMSO and then determined colorimetrically with a Microplate Reader (490 nm).

Table 1. Crystal data and structure refinements for **1**–**3**[a,b].

Compounds	**1**	**2**	**3**
Empirical formula	$C_{57}H_{70}Cu_2F_3N_9O_{51}Si_1W_{12}$	$C_{64}H_{72}Cu_2F_4N_{12}O_{52}SiW_{12}$	$C_{76}H_{94}F_4N_{12}NiO_{54}SiW_{12}$
Formula weight	4115.59	4278.70	4408.60
Wavelength (Å)	0.71073	0.71073	0.71073
Crystal system	Monoclinic	Triclinic	Triclinic
Space group	*P* 21/c	*P*-1	
a (Å)	16.461(13)	10.391(1)	13.8657(16)
b (Å)	20.668(16)	14.0844(13)	14.1504(16)
c (Å)	26.431(2)	17.2130(16)	14.6375(16)
α (deg)	90	112.420(1)	76.511(2)
β (deg)	101.764	98.302(1)	89.181(2)
γ (deg)	90	94.543(1)	76.044(2)
V (Å^3)	8803(2)	2279(4)	2707.6(5)
Z	4	1	1
D_{calc} (mg/m^3)	3.629	3.111	3.468
F(000)	7200	1912	2499
Goodness-of-fit on F^2	1.012	1.079	0.986
Final *R* indices $[I>2\sigma(I)]$	R_1 = 0.0549, wR_2 = 0.1213	R_1 = 0.0509, wR_2 = 0.1456	R_1=0.0905, wR_2=0.2262
R indices (all data)	R_1 = 0.1236, wR_2 = 0.1485	R_1 = 0.0771, wR_2 = 0.1764	R_1 = 0.1190, wR_2 = 0.2443

[a]$R_1 = \sum||F_o| - |F_c||/\sum|F_o|$; [b]$wR_2 = \sum[w(F_o^2 - F_c^2)^2]/\sum[w(F_o^2)^2]^{1/2}$.

Subcultured SGC7901 and SMMC7721 cells were suspended in 0.25% trypsin, respectively. The cell suspension (*ca.* 10^5–10^6 cells mL) was added to a 96-well plate (100 μL per well) and incubated at 37 °C in a 5% CO_2 incubator for 24 h. About 100 μL samples containing the compounds were then added. After 72 h, 20 μL MTT solution (5 mg mL^{-1} in 0.01 M PBS (phosphate buffer solution)) was added, and the mixture allowed to incubate for 4 h. The supernatant was removed and DMSO (150 μL) was added. The resulting mixture was shaken for 10 min at room temperature, and colorimetric analysis was used to examine the cell survival rate. These samples containing three new compounds and parent $H_4SiW_{12}O_{40}$ were obtained by dissolving these compounds in DMSO, autoclaving and diluting by a RPMI 1640 medium to a final concentration of 100, 50, 25, 12.5, 6.25, 3.125, 1.56, and 0.78 μg mL^{-1}.

3. Results and discussion

3.1. *Crystal structures*

$[SiW_{12}O_{40}]^{4-}$ (abbreviated to SiW_{12}) polyoxoanions are the inorganic building blocks in **1–3**, which possess classical α-Keggin structure and contain four W_3O_{13} units and one $[SiO_4]^{4-}$ in the center. Valence sum calculations [25] show that tungstens are +VI oxidation states and Cu and Ni are +II. These results are consistent with elemental analyzes, coordination geometries, crystal color, and charge balance.

3.1.1. Structure description of 1. Single-crystal X-ray structural analysis reveals that **1** is constructed by one SiW_{12}, two crystallographically unique copper cations, three unique Enro molecules and two waters, as shown in figure 1. The parent SiW_{12} coordinates with

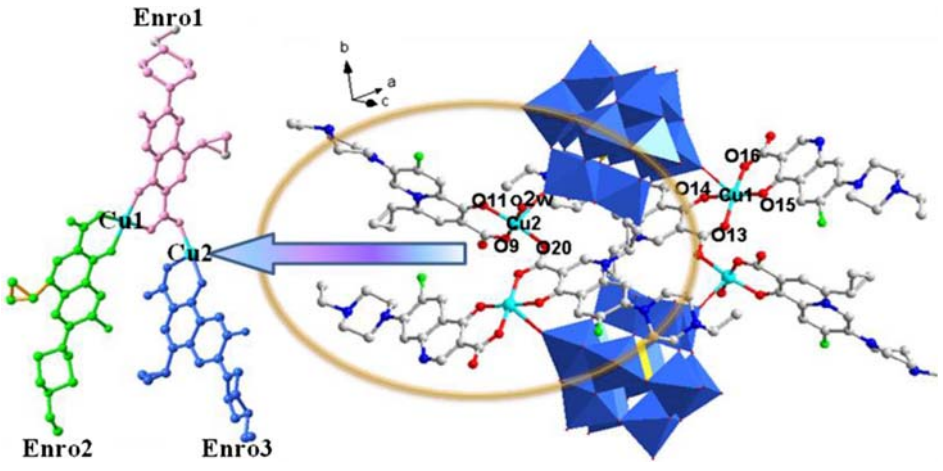

Figure 1. Combined polyhedral and ball/stick representation of the molecular structure unit of **1**. All hydrogens and waters have been omitted for clarity.

Cu1 and Cu2 in a bidentate coordination. Cu–O distances are 2.398 and 2.587 Å. Two crystallographically independent Cu centers show five-coordinate square pyramidal coordination geometries: Cu1 with four oxygens from Enro (Enro1 and Enro2) and one terminal oxygen from SiW_{12}; Cu2 with two oxygens from Enro3, one oxygen from Enro1, one terminal oxygen from SiW_{12}, and one coordinated water. As a result, $\{[Cu_2(Enro)_3H_2O][SiW_{12}O_{40}]\}_2$ forms. A series of structures have shown that intermolecular interaction is a useful synthon in control of the stacking of crystalline lattices [26,27]. Neighboring $\{[Cu_2(Enro)_3H_2O][SiW_{12}O_{40}]\}_2$ dimers are connected forming the POM-drug hybrid 1D supramolecular chains along the *a*-axis via π···π stacking interactions (the centroid···centroid distances between Enro1 and Enro2 are *ca.* 3.8 Å) shown in figure 2. Short interactions among subunits and water stabilized the structure.

3.1.2. Structure description of 2. Single-crystal X-ray structural analysis reveals that **2** is constructed from one SiW_{12}, two copper cations and four Norf molecules, as shown in figure 3. Similar to **1**, SiW_{12} coordinates with two Cu ions (Cu1) in a bidentate

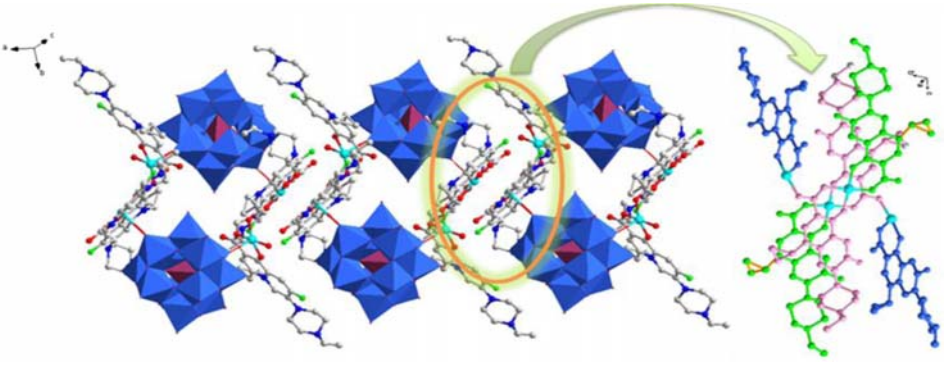

Figure 2. POM-drug hybrid 1D supramolecular chain.

coordination Cu–O distances of 2.557 Å. There is one crystallographically independent Cu center, with square pyramidal coordination geometry completed by four oxygens from two Norf molecules and one terminal oxygen from SiW_{12}. As a result, neutral $[Cu_2(Norf)_4][SiW_{12}O_{40}]$ subunits are obtained. Adjacent subunits are linked to POM-drug hybrid 1-D supramolecular chains via Cu1–O26 (2.875 Å); the 3-D structure is stabilized through short interactions (N6–H–O14 = 2.908 Å; N6–H–O22 = 2.917 Å; N2–H–O27 = 2.741 Å; N2–H–O28 = 2.684 Å) shown in figure 4.

3.1.3. Structure description of 3. Single-crystal X-ray structural analysis reveals that **3** is constructed from one SiW_{12}, one nickel and four Enro molecules as shown in figure 5 (a). Similar to **1** and **2**, the SiW_{12} coordinate with two Ni ions in a bidentate coordination with Ni-O distances of 2.2115 Å. Different from **1** and **2**, Ni1 exhibits octahedral coordination completed by four oxygens from two Enro molecules and two terminal oxygens from two SiW_{12} polyoxoanions (figure 5(b)), resulting in a POMs-drug hybrid 1D chain ($\{[Ni(Enro)_2][SiW_{12}O_{40}]\}_n^{2n+}$). Lattice waters connect neighboring POMs-drug hybrid chains forming the 2D supramolecule (figure 5(c)). Finally, dissociative Enro crystallizes among the 2D-layer and further stabilizes the ultimate structure via short interactions (O27–H–C24 = 2.698 Å; O17–H–C8 = 2.501 Å; C39–H–O10 = 2.877 Å; C25–O27 = 3.135 Å; C26–O27 = 2.896 Å) (figure 5(d)).

3.2. *XRPD characterization, FT-IR spectra, TG-DTA analysis*

The XRPD patterns for **1–3** are presented in figure S1. The diffraction peaks of both simulated and experimental patterns match well, indicating that the phase purities of **1–3** are good. The difference in reflection intensities between simulated and experimental patterns is due to different orientation of the crystals in the powder samples. IR spectra for **1–3** (figures S2–S4) exhibit three characteristic asymmetric vibrations for ν(Si–O), ν(W–O_d)

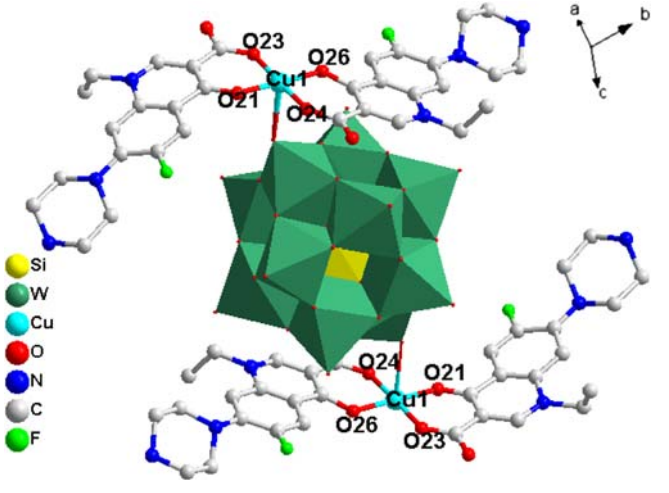

Figure 3. Combined polyhedral/ball/stick representation of the molecular structure unit of **2**. All hydrogens have been omitted for clarity.

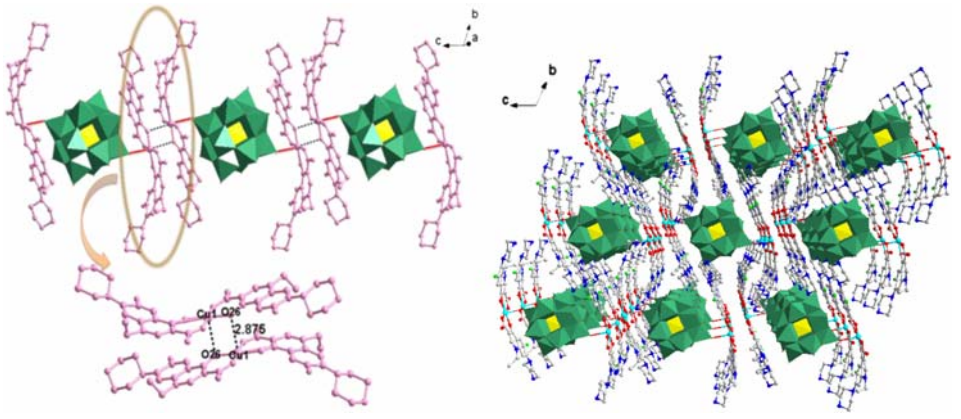

Figure 4. POM-drug hybrid 1D supramolecular chain (left) and 3D supramolecular structure (right).

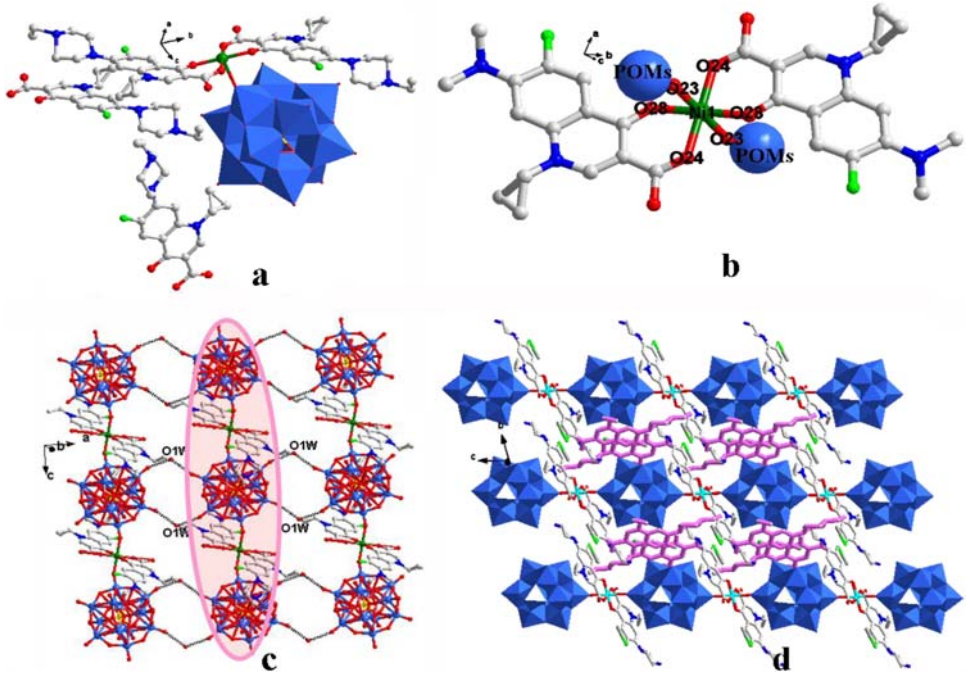

Figure 5. Combined polyhedral and ball/stick representation of the molecular structure unit. All hydrogens have been omitted for clarity (a); coordination mode of metal center (b); 2D supramolecular structure formed by 1D POM-drug hybrid chain and lattice water (c) and 3D supramolecular structure of **3** (d).

and ν(W–$O_{b/c}$–W) at 978, 918, 791 cm^{-1} for **1**, 972, 926, 794 cm^{-1} for **2**, and 972, 926, 791 cm^{-1} for **3** (O_d = terminal oxygen, O_b = bridged oxygen of two octahedra sharing a corner, O_c = bridged oxygen of two octahedra sharing edge), respectively. These data show that the polyoxoanions retain the basic Keggin structure, with a little distortion due to coordination. Bands at 1630–1030 cm^{-1} are associated with Enro and Norf.

To characterize the thermal stabilities, their thermal behaviors were studied by TG-DTA (figure S5). The experiment was performed on crystalline samples under air. For **1**, the

thermal analysis gives a total loss of 27.11% from 200 to 430 °C, which agrees with the calculated weight loss of 27.05% arising from decomposition of water and Enrofloxacin. Weight losses at 330, 380, and 405 °C are followed by strong exothermic peaks in DTA curves, corresponding to decomposition of organic molecules. For **2**, the thermal analysis is similar to that of **1**, giving a total loss of 29.83% from 200 to 450 °C, which agrees with the calculated weight loss of 29.75% arising from decomposition of Norfloxacin. All weight losses at 410 °C are followed by strong exothermic peaks in DTA curves. For **3**, thermal analysis gives a total loss of 33.39% from 200 to 600 °C, which agrees with calculated weight loss of 33.35% arising from decomposition of water and Enrofloxacin. All weight losses at 360, 480, and 415°C are followed by strong exothermic peaks in DTA curves, corresponding to decomposition of organic molecules. These results further confirm the formulas of the compounds.

3.3. *Antitumor activity studies*

A comparison of the antitumor activity for **1–3** and their parent SiW_{12} cluster was made (see table S4). The inhibitory effects against SGC7901 and SMMC7721 lines show that **3** exhibits good antitumor activity and the values of the inhibitory effective cell 50% lethal concentration (IC50) are 0.144 mg/mL for SGC7901 and 0.320 mg/mL for SMMC7721, while **1** and **2** and their parent SiW_{12} show no anti-SGC7901 and anti-SMMC7721 activities as shown in figure 6. This can be reasonably explained by modifying chemistry of POMs. The SiW_{12} polyoxoanions are modified by Cu-quinolone subunits in **1** and **2**, and the Ni-quinolone subunits in **3** with the Cu centers in **1** and **2** adopting five-coordinate pyramidal coordination geometries, which makes against the electron transfer between quinolone and POMs, while Ni centers in **3** adopt six-coordinate geometries and link adjacent POMs forming a 1-D chain structure, which favors electron transfer between quinolone and POM. Thus, electronic distribution, polarity, and redox potentials of POMs can be ameliorated, and the recognition and reactivity of POMs with target biological macromolecules can be altered resulting in enforcement of their antitumor activity. Antitumor activity may rest on the differences of metal ions, namely, the metal ions may differently affect electron transfer between quinolone and POMs.

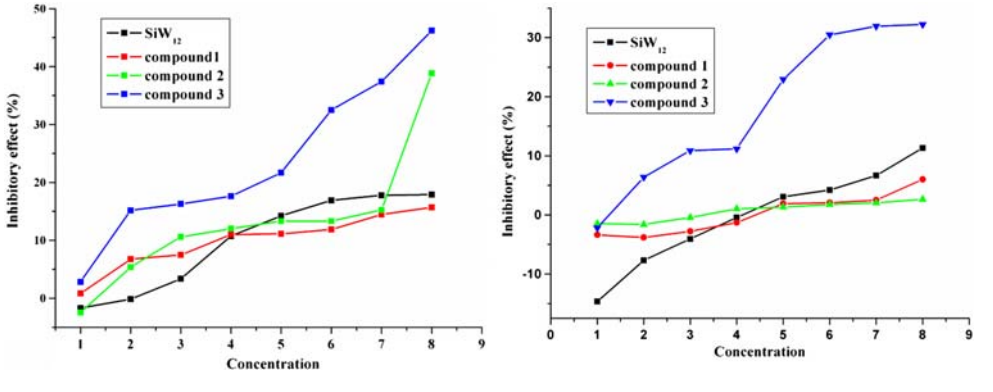

Figure 6. Curve of the anti-tumor activity against SGC7901 (left) and SMMC7721 (right) for **1**-**3** and the parent SiW_{12} cluster (concentration: 1, 2, 3, 4, 5, 6, 7 and 8 represent 0.78, 1.56, 3.125, 6.25, 12.5, 25, 50 and 100 $\mu g \cdot mL^{-1}$, respectively).

4. Conclusions

Three TM-quinolone-SiW_{12} based compounds were obtained and structurally characterized. MTT investigations find that **3** possesses better antitumor activity than the parent **1** and **2**, due to the differences of metal ions, which result in different electron transfer between quinolone and POMs. Combined with reported work, we deduce that the changes of antitumor properties come from the synergism of POMs, metal ions and, drug molecules. So successful isolation of the three compounds is helpful to extend applications of POMs in medicine, and more work needs to be done about the TM-drugs-POMs reaction system to explore the possible effect of drug molecules modifying POM clusters.

Supplementary material

CCDC (891387, 891388, 891389) contains the supplementary crystallographic data for **1**–**3**, respectively. These data can be obtained free of charge via http://www.ccdc.cam.ac.uk/conts/retrieving.html, or from the Cambridge Crystallographic Data Centre, 12 Union Road, Cambridge CB2 1EZ, UK; Fax: +44 1223 336 033; or Email: deposit@ccdc.cam.ac.uk. Tables of selected bond lengths (Å), bond angles (deg) and IR for **1**–**3** are provided in supporting information.

Acknowledgements

This study is financially supported by the National Natural Science Foundation (Grant No. 21271089), the Scientific and technological innovation team (2012TD010) and Postdoctoral Foundation in Heilongjiang Province.

References

[1] M.T. Pope. *Heteropoly and Isopoly Oxometalates*, Springer-Verlag, Berlin (1983).
[2] M.T. Pope, A. Müller. *Angew. Chem. Int. Ed. Engl.*, **30**, 3448 (1991).
[3] C.L. Hill. *Chem. Rev.*, **98**, 1 (1998).
[4] Q. Chen, J. Zubieta. *Coord. Chem. Rev.*, **114**, 107 (1992).
[5] D.L. Long, E. Burkholder, L. Cronin. *Chem. Soc. Rev.*, **36**, 105 (2007).
[6] P.P. Mishra, J. Pigga, T.B. Liu. *J. Am. Chem. Soc.*, **130**, 1548 (2008).
[7] S.D. Jiang, B.W. Wang, G. Su, Z.M. Wang, S. Gao. *Angew. Chem., Int. Ed.*, **10**, 1736 (2010).
[8] T. Ishida, M. Nagaoka, T. Akita, M. Haruta. *Chem. Eur. J.*, **14**, 8456 (2008).
[9] X. Wang, J. Liu, M.T. Pope. *Dalton Trans.*, 957 (2003).
[10] W. Rozenbaum, D. Dormont, B. Spire, E. Vilmer, M. Gentilini, L. Montagnier, F.B. Sinoussi, J.C. Chermann. *Lancet*, 450 (1985).
[11] J. Li, Y.F. Qi, J. Li. *J. Coord. Chem.*, **57**, 1309 (2005).
[12] H. Zhang, Y. Lan, L.Y. Duan. *J. Coord. Chem.*, **56**, 85 (2003).
[13] J. Li, J. Li, Y.F. Qi, H.F. Wang, E.B. Wang, C.W. Hu, L. Xu, X.Y Wu. *Chem. J. Chin. Univ.*, **25**, 1010 (2004).
[14] W.F. Bu, L.X. Wu, X. Zhang, A.C. Tang. *J. Phys. Chem. B*, **107**, 13425 (2003).
[15] H.Y. An, D.R. Xiao, E.B. Wang, C.Y. Sun, Y.G. Li, L. Xu. *J. Mol. Struct.*, **751**, 184 (2005).
[16] K.J. Huang, X. Liu, W.Z. Xie, H.X. Yuan. *Colloids Surf. B*, **64**, 269 (2008).
[17] S.A. Sadeek, W.H. El-Shwiniy. *J. Coord. Chem.*, **63**, 3471 (2010).
[18] M. Patel, D. Gandhi, P. Parmar. *J. Coord. Chem.*, **64**, 1276 (2011).
[19] H. Muslu, A. Golcu, M. Tumer, M. Ozsoz. *J. Coord. Chem.*, **64**, 3393 (2011).
[20] J.Q. Sha, L.Y. Liang, X. Li, Y. Zhang, H. Yan, G. Chen. *Polyhedron*, **30**, 1657 (2011).

[21] J.Q. Sha, X. Li, Y.H. Zhou, P.F. Yan, G.M. Li, C. Wang. *Solid State Sci.*, **13**, 1972 (2011).
[22] J.Q. Sha, L.Y. Liang, P.F. Yan, G.M. Li, C. Wang, D.Y. Ma. *Polyhedron*, **31**, 422 (2012).
[23] (a) G.M. Sheldrick, *SHELX-97, Program for Crystal Structure Refinement*, University of Göttingen, Göttingen (1997); (b) G.M. Sheldrick, *SHELXL-97, Program for Crystal Structure Solution*, University of Göttingen, Göttingen (1997).
[24] X.H. Wang, J.F. Liu, Y.G. Chen, Q. Liu, J.T. Liu, M.T. Pope. *J. Chem. Soc., Dalton Trans.*, 1139 (2000).
[25] I.D. Brown, D. Altermatt. *Acta Crystallogr., Sect. B*, **41**, 244 (1985).
[26] E. Corradi, S.V. Meille, M.T. Messina, P. Metrangolo, G. Resnati. *Angew. Chem., Int. Ed. Engl.*, **39**, 1782 (2000).
[27] Z.G. Han, Y.L. Zhao, J. Peng, C.J. Gómez-García. *Inorg. Chem.*, **46**, 5453 (2007).